Two nuclear localization signals regulate intracellular localization of the Duck enteritis virus UL13 protein

Linjiang Yang
Sichuan Agriculture University
Xixia Hu
Sichuan Agriculture University
Anchun Cheng (chenganchun@vip.163.com)
Sichuan Agricultural University https://orcid.org/0000-0001-6093-353X
Mingshu Wang
Sichuan Agriculture University
Renyong Jia
Sichuan Agriculture University
Qiao Yang
Sichuan Agriculture University
Ying Wu
Sichuan Agriculture University
Shun Chen
Sichuan Agriculture University
Mafeng Liu
Sichuan Agriculture University
Dekang Zhu
Sichuan Agriculture University
Xumin Ou
Sichuan Agriculture University
Xingjian Wen
Sichuan Agriculture University
Sai Mao
Sichuan Agriculture University
Di Sun
Sichuan Agriculture University
Shaqiu Zhang
Sichuan Agriculture University
Xinxin Zhao
Sichuan Agriculture University
Juan Huang
Sichuan Agriculture University
Qun Gao
Sichuan Agriculture University
Yunya Liu
Sichuan Agriculture University
Yanling Yu
Sichuan Agriculture University
Ling Zhang

Sichuan Agriculture University
Bin Tlan
Sichuan Agriculture University
Leichang Pan
Sichuan Agriculture University
Mujeeb Ur Rehman
Sichuan Agriculture University
Xiaoyue Chen
Sichuan Agriculture University

Research article

Keywords: Duck enteritis virus, Conserved herpesvirus protein kinase, UL13, NLS

Posted Date: February 29th, 2020

DOI: https://doi.org/10.21203/rs.3.rs-15523/v1

Version of Record: A version of this preprint was published at Poultry Science on January 1st, 2021. See the published version at https://doi.org/10.1016/j.psj.2020.09.069.

Abstract

Background

UL13 multifunctional tegument protein of duck enteritis virus (DEV) is predicted as protein kinase (CHPK); however, little is known concerning its subcellular localization signal.

Results

In this study, by transfection with two predicted nuclear signals of DEV UL13 fused to enhanced green fluorescent protein (EGFP), two bipartite nuclear localization signal (NLS) was identified. We identified the nuclear localization signals (NLSs) that control its nuclear importing using fluorescence assay and proved that nuclear localization of DEV UL13 is a classical importin α/β-dependent process. And we constructed the mutant DEV, with the NLSs of UL13 deleted, to explore whether it will affect the replication of virus particles.

Conclusions

DEV UL13 protein is directed by amino acids 4 to 7 and 90 to 96, and proved that this nuclear import occurs via the classical importin α/β-dependent process. And Entry nucleus of UL13 protein has no effect on DEV replication in cell culture. Our study enhances the understanding of DEV pUL13. Taken together, these results would provide significant information for the stud y of the biological function of UL13 during DEV infection.

Background

DEV, a member of the Alphaherpesvirinae subfamily, can cause serious clinical symptoms and pathological changes, such asvascular injury, tissue haemorrhage, gastrointestinal mucosal papulosis-like lesions, and degeneration of lymphoid and parenchymal organs [1–3]. Also, DEV can lead to acute, fever, septicemia and infectious diseases in ducks, geese, swans and other birds. The morbidity and mortality of infected or unprotected ducks are as high as 100%. The disease often trigger severe economic losses to the global waterfowl industry [4].

According to the Ninth International Committee on Taxonomy of Viruses (ICTV), Duck enteritis virus (DEV) is classified into the subfamily Alphaherpesvirinae of the family Herpesviridae [5]. DEV infection, known as duck plague (DP) or duck viral enteritis (DVE), is among the most widespread and devastating diseases of waterfowl [6]. DEV is a linear double-stranded DNA virus that contains 78 open reading frames. The UL13 gene of DEV, which is predicted to encode a Ser/Thr protein kinase (CHPKs), was previously identified by our group [7–8]. Amino acid sequence analysis showed that the UL13 protein kinase shows more than 35% similarity with reported CHPK, and the exploration of DEV UL13 will not only offer data about the molecular biological characteristics of DEV but also supplement our knowledge of the characteristics and functions of the CHPK family.

CHPKs can both autophosphorylate and phosphorylate certain viral and cellular proteins that help the virus to replicate and spread, with many activities occurring in the nucleus. For example, CHPKs have been reported to participate in the phosphorylation of nuclear lamina components to facilitate the nuclear egress of progeny capsids [9–14]. In addition to roles in nuclear egress, CHPKs have been proven to have other effects in the nucleus that may influence viral replication and the cell cycle. CHPKs affect the efficiency of virus replication by phosphorylating DNA polymerase processivity factors, such as UL44 of HCMV and BMRF1 of EBV [15, 16], histones [17], and RNA polymerase II [18, 19], to promote viral DNA replication and protein expression. In recent years, the EBV BGLF4 protein has been demonstrated to inhibit cell cycle G1/S progression and induce chromosomal abnormality [20, 21]. Moreover, HSV-1 UL13 has been found to stimulate the expression of suppressor of cytokine signalling 3 (SOCS-3), a negative regulator of IFN, to escape the interferon response. It has also been reported that CHPKs of HCMV, EBV, KSHV, and murine herpesvirus-68 (MHV-68) can subvert the type I IFN response by inhibiting the activity of interferon regulatory factor 3 (IRF-3) [22–24]. Furthermore, some, but not all, CHPKs in Betaherpesvirinae and Gammaherpesvirinae can phosphorylate antiviral nucleoside analogue ganciclovir (GCV) [25–29], which is also present in the nucleus.

The characteristics of some genes from DEV had been reported by our team [30–56]. However, the function of DEV UL13 protein has rarely been reported to date. Certain of characteristics of DEV UL13 protein have been identified in our previous study. This

report will complement the location characteristic of DEV UL13 and lay the foundation for its functional exploration in the nucleus.

Results

Localization of recombinant UL13 and UL13-△NLSs mutated protein in transfected DEFs

We have proved that UL13 protein of DEV also can enter into nucleus. PSORT II Prediction revealed amino acids 4 to 7 (Arg-Arg-Arg-Arg) and 90 to 96 (Pro-Gly-Lthoys-Arg-Lys-Thr-Lys), as basic amino acid patches, as putative NLSs (Figure S1). To examine the function of these predicted NLSs, we constructed mammalian expression plasmids for UL13-GFP fusion proteins or proteins with NLS1 or/and NLS2 deleted (Fig. 1A) and transfected them into DEFs. Compared with that the fluorescence of UL13-GFP fusion proteins located both in nucleus and cytoplasm (Fig. 1B b, g, l), when NLS1 or NLS2 was deleted, the majority of the fluorescence displayed a cytoplasmic distribution in DEFs (Fig. 1B c, h, m, d, i, n). Furthermore, the UL13-GFP fusion protein, with NLS1 and NLS2 both deleted, exhibited a completely cytoplasmic distribution (Fig. 1B e, j, o). We also analyse the nuclear compartmentalization of UL13/UL13-△NLSs. As shown in Fig. 1C, the nuclear/cytoplasmic fluorescence ratio of the UL13-△NLS1&NLS2 protein was significantly decreased compared to the UL13 protein (P□0.01), and both the UL13-△NLS1 and UL13-△NLS2 proteins were also significantly decreased (P□0.001). The decrease in the nuclear/cytoplasmic fluorescence ratio was higher for UL13-△NLS1&NLS2 than for UL13-△NLS1 and UL13-△NLS2. All these results suggested that both NLS1 and NLS2 are responsible for the nuclear localization of DEV UL13 and work together to enhance this functionality. We also separated the cytoplasmic and nuclear proteins expressed from pEGFP-N1-UL13 or pEGFP-N1-UL13-△NLS1&△NLS2 plasmids in DEF cells, and analysed the quantity of UL13 protein distributed in the cytoplasm and nucleus via western blotting (Fig. 1D). Compared with the distribution of the UL13 protein expressed in the pEGFP-N1-UL13 group, the ratio of UL13 protein in the nucleus in the pEGFP-N1-UL13-△NLS1 &△NLS2 group was significantly reduced. We used β-actin and Lamin A/C as controls for these cytoplasmic/nuclear fractions.

Localization of the NLS-GFP fusion protein in transfected DEFs

To further examine whether NLS1 and NLS2 can import heterologous proteins into the nucleus, sequences encoding NLS1 and NLS2 were fused to GFP to obtain NLS1-GFP, NLS2-GFP, and NLS1&NLS2-GFP recombinant plasmids and transfected into DEFs (Figure 2A). Fluorescence assays showed a greater proportion of the NLS1-GFP and NLS2-GFP fusion proteins in the nucleus than in the cytoplasm (Figure 2B b, f, j, c, g, k); in contrast, NLS1&NLS2-GFP showed a predominantly nuclear distribution (Figure 2B d, h, l), and GFP alone showed a homogeneous distribution (Figure 2B a, e, i). We also analysed differences in the nuclear and cytoplasmic fluorescence ratios between GFP and NLSs-GFP and found that the nuclear/cytoplasmic fluorescence ratios for NLS1-GFP, NLS2-GFP and NLS1&NLS2-GFP were significantly increased compared to GFP (P□0.001) (Figure 2C), with that of NLS1&NLS2-GFP being particularly increased. We also separated the cytoplasmic and nuclear proteins expressed from NLS1-GFP or NLS2-GFP plasmids in DEF cells, and analysed the quantity of UL13 protein distributed in the cytoplasm and nucleus via western blotting (Figure 2D). Compared with the distribution of the UL13 protein expressed in the nucleus, the ratio of UL13 protein in the cytoplasm in the NLS1-GFP or NLS2-GFP group was significantly reduced.

Our results confirmed that both NLS1 and NLS2 of DEV UL13 act as nuclear localization signals. Each could mediate protein entry into the nucleus, and their combination increased the function of the nuclear localization signal.

The effects of nuclear import inhibitors on the location of DEV UL13

NLS1 and NLS2 of DEV UL13 are predicted to be pat4 and pat7 monopartite prototypical nuclear localization signals, respectively. It has been reported that ivermectin blocks importin α and β interaction and inhibits the nuclear transport facilitated by the prototypical NLS-mediated mechanism, with no effect on proteins containing NLSs recognized by alternative nuclear import pathways or other nuclear import pathways. Therefore, we tested whether the nuclear import of the DEV UL13 protein requires the interaction of importin α and β by treating DEF cells transfected with pEGFP-N1-UL13 recombinant plasmids with/without

ivermectin. As shown in Figure 3A, less nuclear UL13 protein was found in DEFs treated with ivermectin than DEFs without ivermectin treatment at 16h post-transfection (Figure 3A a, g, m, b, h, n). The nuclear distribution of NLS1&NLS2-GFP with ivermectin treatment was also reduced compared to the no treatment group (Figure 3A c, i, o, d, j, p), whereas there was no change in the distribution of GFP alone with/without ivermectin treatment (Figure 3A e, k, q, f, l, r). We also analysed differences in the nuclear and cytoplasmic fluorescence ratio of NLS1&NLS2-GFP and UL13 in DEF cells with or without ivermectin treatment and found that the ratio of UL13 declined significantly($P<0.001$), with the mean ratio of the NLS1&NLS2-GFP group reduced from 0.8 to 0.4 after ivermectin treatment. Statistical analysis showed that the nuclear accumulation of NLS1&NLS2-GFP and UL13 was significantly impaired by ivermectin (Figure 3B) ($P<0.01$). These results suggested that the nuclear import of DEV UL13 occurs by the classical transport process that requires the interaction of importin α and β and is mediated by the NLSs of DEV UL13.

Entry nucleus of UL13 protein has no effect on DEV replication in cell culture

To examine the effect of entry nucleus of UL13 protein on viral proliferation, we constructed DEV CHv-UL13ΔNLS, which was a mutant of both NLS1 and NLS2 of DEV UL13 being deleted, and DEV CHv-UL13ΔNLS R (a revertant) (Figure 4A). By RFLP analysis and sequencing, we determined that the DEV CHv-UL13ΔNLS and DEV CHv-UL13ΔNLS R recombinant viruses were mutated only at their appropriate target site (Figure 4B).

A plaque assay indicated that the DEV CHv-UL13ΔNLS could grow in DEF, and the difference of plaque size between DEV CHv-UL13ΔNLS and DEV CHv has no significance (Figure 5A). The growth curve of DEV CHv-UL13ΔNLS exhibited the same trend of DEV CHv in both the supernatant and cells during the infection period (Figure 5B). The phenotype of DEV CHv-ΔUL13R exhibited similar

Discussion

All herpesviruses encode serine/threonine kinases, which are involved in viral proliferation and organism immunity [57]. Two types of conserved herpesvirus serine/threonine kinases have been described in Herpesviridae: one is conserved only in the Alphaherpesvirus subfamily, exemplified by the US3 kinase of HSV; the others are CHPKs, which are conserved across the entire family. Studies on CHPKs have mainly focused on function and molecular characteristics, especially for human herpesviruses, whereas studies on CHPKs of animal herpesviruses, such as DEV, are comparatively scarce. In a previous study, our group isolated DEV, which was grouped into Alphaherpesvirinae, from the intestine of a sick duck and sequenced the genome. This analysis showed that DEV encodes a UL13 protein showing 35 ~ 40% similarity with reported CHPKs in human herpesviruses, and 40 ~ 50% similarity with the CHPK of poultry herpesviruses.

The functions of CHPKs in the nucleus have been well characterized, especially for members of Betaherpesvirinae and Gammaherpesvirinae. In contrast, there are relatively few reports for members of Alphaherpesvirinae to date. Maybe it is associated with another type of herpesvirus protein kinases, which is conserved only in the alphaherpesvirus subfamily, exemplified by the US3 kinase of HSV. It has been reported that UL13 protein participate in the phosphorylation of nuclear lamina components to facilitate the nuclear egress of progeny capsids in cells infected with HSV-2 [13]. However, nuclear egress regulation needs both UL13 and US3 to participate in HSV-1 [14]. In pseudorabies virus (PRV) and Marek's disease virus (MDV), which also belong to alphaherpesvirus subfamily, the capsid nuclear export is a conserved role for US3 kinase [58]. HSV-1 UL13 was found to participate in inducing the expression of a negative regulator of IFN, suppressor of cytokine signalling 3 (SOCS-3), to evade the interferon response [24]. In VZV-infected cell, the US3 ortholog participated in interfering with induction of the IFN signalling pathway following exposure to IFN [59]. And both US3 ortholog and UL13 of VZV can phosphorylate a nuclear transcription regulatory protein, IE62, to promote virion incorporation [60–62]. In HSV-1 / HSV-2 infected cells, UL13 protein is involved in the nucleocapsid out of nucleus. In this chapter, the author proved that the protein of DEV UL13 can enter into the nucleus in the cells infected and transfected by the virus, determined the signal region of UL13 entering into the nucleus through various ways, and preliminarily discussed the mechanism of UL13 entering into the nucleus.

The cell biological characteristics of the successfully constructed and rescued DEV CHV BAC UL13 - Δ NLS infectious clone were analysed. Compared with the parent virus, it was found that there was no significant difference in the formation size of plaque or the growth and replication ability of UL13 - Δ NLS recombinant virus and the parent virus. The results showed that UL13 protein had little effect on virus replication. Among the members of β - herpesvirus subfamily and γ - herpesvirus subfamily, UL13 homologues have been reported to affect virus replication, for example, HCMV UL97 protein kinase affects virus replication by phosphorylating virus DNA polymerase extension factor UL44 [63]. EBV BGLF4 affects virus growth and replication by phosphorylating virus DNA elongation factor BMRF1 [64]. It has been reported that HSV-1 UL13 can promote the expression of a series of viral genes, including ICP22 and some late genes [65], but there is no further report about the effect of UL13 protein on viral replication in the members of α- herpesvirus subfamily. This may be related to the existence of another conserved protein kinase, US3 protein kinase, in the subfamily of alpha herpesvirus. It is reported that US3 protein kinase has an important effect on the growth and replication of virus [66]. We also tested the kinase activity of UL13 - Δ NLS protein in vivo, and found that the DEV UL13 protein without nuclear localization signal can still phosphorylate US3 protein, indicating that the loss of nuclear localization signal has no significant effect on the activity of UL13 protein kinase, but the biological function of DEV UL13 protein in the nucleus needs further study.

Conclusions

In our study, we identified that the nuclear import of DEV UL13 protein is directed by amino acids 4 to 7 and 90 to 96, and proved that this nuclear import occurs via the classical importin α/β - dependent process. We also constructed a mutant virus with NLSs of UL13 deleted, and preliminarily explored characteristics of this mutant virus for further function study.

Methods

Cells and virus

The previously reported DEV CHv strain (Gen Bank No.JQ647509) was maintained in our lab[67–68] and slightly changes. Briefly, duck embryo fibroblasts (DEFs) were propagated in Minimal Essential Medium (MEM, Gibco-BRL, Grand Island, NY, USA) provided by our lab supplemented with 10% (v/v) foetal bovine serum (FBS, Gibco-BRL, Grand Island, NY, USA) and incubated at 37 °C with 5% CO2.

Analysis of sequence motifs within UL13

Putative nuclear localization signals (NLSs) within the UL13 coding sequence were identified using PSORT II Prediction (http://psort.nibb.ac.jp/form2.html) [69]. Sequence analysis using PSORT II predicted that UL13 has two potential NLS in its arginine-rich regions, namely, RRRR at aa 4 to 7 and PGKRKTK at aa 90 to 96 (Fig. 1).

Construction of recombinant plasmids

The experimental operation was carried out as described previously [70–72]. Briefly, the full-length UL13 sequence was PCR amplified from DEV chromosomal DNA using the primers F-UL13F and F-UL13R. UL13-△NLS1 was PCR amplified from DEV chromosomal DNA using the primers △NLS1F and F-UL13R. UL13-△NLS2 was amplified by overlapping PCR from DEV chromosomal DNA using the primers F-UL13F, △NLS2R, △NLS2F, and F-UL13R. UL13-△NLS1&△NLS2 was PCR amplified from pEGFP-N1::UL13-△NLS2 DNA using the primers △NLS1F and F-UL13R (Tables 1). The PCR fragments were purified and digested with EcoRI and HindIII and ligated into the pEGFP-N1 plasmid digested with the corresponding restriction endonucleases. The ligation mixtures were introduced into CaCl2-competent E. coli DH5α cells, and transformants were selected on LB plates containing 50 μg/ml Kan. Clones were screened by PCR with the corresponding primers. The validity of the sequences was determined by sequencing. The GFP, NLS1-GFP, NLS2-GFP and NLS1&NLS2-GFP genes were amplified by PCR from pEGFP-N1 DNA using the primers GFPF and GFPR; NLS1F and GFPR; NLS2F and GFPR; and NLS1&NLS2F and GFPR, respectively (Table 1). These PCR fragments were purified and digested with EcoRI and HindIII. Then, the purified fragments were ligated into the pcDNA3.1(+) plasmid digested with the corresponding restriction endonucleases. Ligation mixtures were introduced into the CaCl2-competent E. coli DH5α strain, and transformants were selected on LB plates containing Amp at 100 μg/ml. Clones were screened by PCR with the corresponding primers. Sequencing was used for confirmation.

Table 1
Oligonucleotide primers used in this work

Oligonucleotide primer	Sequencea (5′-3′)
T-UL13F	GGATCCCTGGTGGCTACGGAGAG
T-UL13R	AAGCTTCCAAGGGCGTATATGTC
F-UL13F	cccAAGCTTATGGCTGGACGAAGACG
F-UL13R	ccgGAATTCTGTTATAAATCCACAATAGAG
△NLS1F	cccAAGCTTATGGCTGGAAGCCCTATTAGCGAAATG
△NLS2R	CATCTACTATCCTTTCTCTCTTTACTG
△NLS2F	GAAAGGATAGTAGATGGAGCCTGG
GFPF	cccAAGCTTATGGTGAGCAAGGGCG
GFPR	ccgGAATTCTGATTATGATCTAGAGTCG
NLS1F	cccAAGCTTATGGCTGGACGAAGACGACGAAGCCCTATGGTGAGCAAGGGCG
NLS2F	cccAAGCTTATGAAGGATCCTGGCAAACGTAAGACAAAGAGTAGAATGGTGAG CAAGGGCG
NLS1&NLS2F	cccAAGCTTATGGCTGGACGAAGACGACGAATGAAGGATCCTGGCAAAC

[a]The sequences of restriction endonuclease sites are in italics, and lowercase letters denote protective bases.

Immunofluorescence assay

The experimental operation was carried out as described previously and slightly change[73–77]. Briefly, Slide-cultured DEF cells were fixed with 4% paraformaldehyde at 16 h post-transfection, permeabilized with 0.1% Triton X-100 and blocked with bovine serum albumin (BSA) for 1 h. The cells were incubated with the rabbit anti-UL13 antiserum (1:200 dilution) for 1 h at 37℃ and then with a goat anti-rabbit antibody conjugated to fluorescein isothiocyanate (FITC, 1:200 dilution, Zhongshan, Beijing, China) for 30 min. The nuclei were stained with DAPI. The cells were observed using a Nikon ECLIPSE 80i microscope.

Extraction and analysis of cytoplasmic/nuclear proteins

The experimental operation was carried out as described previously [78]. Briefly, confluent monolayers of DEF cells were transfected with pEGFP-N1-UL13 or pEGFP-N1-UL13-△NLS1&△NLS2 plasmids (2.5 μg/well) in 6-well plates for 16 h and harvested after washing twice with PBS. The cells were pelleted by centrifugation at 3,000 rpm for 5 min and resuspended in 20 μl cytosol extraction buffer (10 μl 1 M HEPES (pH 7.5); 6 μl 100% Triton X-100; 50 μl 3 M NaCl; 2 μl 0.5 M EDTA; 50 μl 200 μg/ml protease inhibitor; 882 μl ddH20) and incubated for 5 min on ice. The suspension was separated into nuclear and cytoplasmic fractions by 4,000 rpm for 5 min. The nuclear fraction was resuspended in 15 μl nuclear extraction buffer (20 μl 1 M HEPES (pH 7.5); 250 μl 100% glycerol; 140 μl 3 M NaCl; 12 μl 100 mM MgCl2; 4 μl 0.5 M EDTA; 5 μl 1 M DTT; 50 μl 200 μg/ml protease inhibitor; 527.1 μl ddH20) and incubated for 30 min on ice, meanwhile, strongly mixed by vertexing six times for 30 s. The supernatant was collected by centrifugation for 30 min at 14,000 rpm at 4℃. The obtained cytoplasmic/nuclear proteins were subjected to western blotting according to the protocol described above. The anti-UL13 antibody, rabbit anti-β-actin antibody (APGBIOLtd, Shanghai, China) and rabbit anti-Lamin A/C antibody (Signalway Antibody, Maryland, USA) were used as primary antibody, separately. Protein bands were visualized by using ECL Western blotting detection reagents (Bio-Rad, California, USA) according to the manufacturer's instructions.

Analysis of pharmaceutical inhibition of nucleus/cytoplasm transport

The experimental operation was carried out as described previously [79–80]. Briefly, DEFs were cultured in MEM supplemented with 10% (v/v) FBS at 37 °C with 5% CO2. Lipofectamine 2000 was used according to the manufacturer's instructions to transfect the pEGFP-N1-UL13 or pcDNA3.1(+)-NLS1&NLS2-GFP recombinant plasmid (2.5 μg per well) into DEFs in 6-well cell culture plates. Where appropriate, cells were treated with ivermectin at a final concentration of 25 μM for 1 h before imaging [81–83]. Cells were

imaged live at 16 h after transfection using a Nikon ECLIPSE 80i microscope. To determine the nuclear/cytoplasmic fluorescence ratio, digitized images were analysed using the Image-Pro Plus software. Statistical analysis was performed using the GraphPad Prism 6.0 software.

Construction of Recombinant Viruses DEV CHv-UL13ΔNLS

To create the DEV CHv-UL13ΔNLS virus, with both NLS1 and NLS2 of UL13 deleted, we need to create the UL13 and UL14 gene-deleted recombinant mutant, DEV CHv-ΔUL13&UL14 virus first according to the overlapping of UL13 gene and UL14 gene regions. The target segment (UL13 left arm-FRT-Kan-FRT-UL14 right arm) was PCR-amplified using the ΔUL13&UL14 F F/R primers (Table 2). Then, the infectious clone DEV CHv-ΔUL13&UL14-G was generated by employing a recombinating system based on the genetic manipulation of the DEV CHv-G infectious clone[34–37]. Briefly, the pKD46 plasmid, which encodes the recombination genes exo, beta, and gam under the tight control of a ParaB promoter, was first introduced into E. coli DH10B containing the DEV CHv-G plasmid by electrophoretic transfer. In this system, the UL13&UL14 coding sequence was replaced by the target segments amplified from the pKD4 plasmid. Next, the pCP20 plasmid was transferred into the above cells, which contain DEV CHv-ΔUL13&UL14-G and kanamycin-resistant gene cassette. Removal of the kanamycin-resistant cassette was accomplished by incubation at 30◦C for 8 h then at 42◦C overnight. Then we generated the DEV CHv-UL13ΔNLS-G and the revertant, DEV CHv-UL13ΔNLS R-G based on the same method used above but with two different target segments. Target segment of DEV CHv-UL13ΔNLS-G, UL13ΔNLS-UL14-FRT-Kan-FRT-UL14 right arm, which was fusion PCR-amplified using the UL13-ΔNLS F1X/UL13-ΔNLS R1, UL13-ΔNLS F2/ΔUL13(K179M) R and FRT-Kan F/ R primers (Table 2) with the pEGFP-N1:: UL13-△NLS1&△NLS2 plasmids, the CHv genome and the pKD4 plasmid as template, respectively; target segment of DEV CHv-UL13ΔNLS R-G, UL13-UL14-FRT-Kan-FRT-UL14 right arm, using the UL13-ΔNLS F1/ΔUL13(K179M) R and FRT-Kan F/ R primers (Table 2) with the CHv genome and the pKD4 plasmid as template, respectively. The DEV CHv-UL13ΔNLS-G and DEV CHv-UL13ΔNLS R-G infectious clones, were identified by sequencing and RFLP analysis. Finally, the DEV CHv-UL13ΔNLS and DEV CHv-UL13ΔNLS R recombinant viruses were rescued; freshly prepared DEV CHv-UL13ΔNLS -G and DEV CHv-UL13ΔNLS R-G plasmids were transfected into DEFs for one to 10 d, and the cells were examined by fluorescence microscopy until greenfluorescence protein seemed sufficiently expressed, at which point, they were harvested after freeze-thawing 3 times. After amplifying the DEV CHv-UL13ΔNLS and DEV CHv-UL13ΔNLS R viruses, viral PCR identification and sequencing of the target region were performed (Table 1).

Table 2
Primers used for Red recombination to construct the CHv-BAC-UL13-Δ NLS

Oligonucleotide primer	Sequence (5′-3′)
pKD46 F	AAAGCCGCAGAGCAGAAGGTGG
pKD46 R	GGTAAACGGGCATTTCAGTTCAAGG
ΔUL13&UL14 F	ATATGATTTGTTTTTTCCTACTCTATTGAATAGTGCGCACTCTCGCTAACGTGTAGGCTGGAGCTGCTTC
ΔUL13&UL14 R	ACGTTTGCAGTGATGTACTGGCGATGAGCTACCATCTATATCCCCACTCATGGTAGCATATGAATATCCTCCTTAG
UL13-ΔNLS F1	CTTCACATAATACGCCACTGATC
UL13-ΔNLS F1X	GGCGAAAGGCTGCAATACG
UL13-ΔNLS R1	CCGATAGGATTCATTTCGCTAATAGGGCTTCCAGCCATTCGTTACCAGATAGTC
UL13-ΔNLS F2	GACTATCTGGTAACGAATGGCTGGAAGCCCTATTAGCGAAATG AATCCTATCGG
ΔUL13(K179M) R	TTAGTTATAAATCCACAATAGAG
FRT-Kan F	AGAAGCGCCGCTCCTCTATTGTGGATTTATAACTAAGTGTAGGCTGGAGCTGCTTC
FRT-Kan R	ACGTTTGCAGTGATGTACTGGCGATGAGCTACCATCTATATCCCCACTCATGGTAGCATATGAATATCCTCCTTAG

Plaque Assay

The experimental operation was carried out as described previously [84–85]. Briefly, DEFs were incubated with DEV CHv, DEV CHv-UL13ΔNLS, or DEV CHv-UL13ΔNLS R at 37◦C for 2 hours. The plates were then overlaid with an equal-parts mixture of 2 × MEM and 0.5% methylcellulose (9004-67-5, J & K SCIENTIFIC LTD., Beijing, China) after discarding unabsorbed particles. After incubation at 37◦C for 6 d, the cells were fixed with 4% paraformaldehyde and stained with 0.05% crystal violet (C3886, Haoran Bio, Beijing, China). Plaque areas were then measured with ImagePro Plus software, with 50 plaques chosen at random for each virus.

Growth Curve Assay

The experimental operation was carried out as described previously and slightly changes [86]. Briefly, duck embryo fibroblasts cells were infected with DEV CHv, DEV CHv-UL13ΔNLS, or DEV CHv-UL13ΔNLS R at 200 TCID50. The cells were maintained in MEM supplemented with 2% FBS, and samples of the cells and supernatants were separately harvested at 6, 12, 24, 48, 72, and 96 h for the growth curve assay after being freeze-thawed 3 times. The growth curve was recorded via measuringtheTCID50,whichwascalculatedwiththeReedMuench method, of the samples at different time points and triplicate experiments were performed.

List Of Abbreviations

Abbreviation	Full name
DEV	Duck enteritis virus
CHPK	Conserved herpesvirus protein kinase
NLS	Nuclear localization signals
HSV	Herpes simplex virus
HCMV	Human cytomegalovirus
KSHV	Kaposi's sarcoma-associate herpesvirus
DEF	Duck embryo fibroblasts
PRV	Pseudorabies virus
MDV	Marek’s disease virus
SOCS-3	Suppressor of cytokine signalling 3
Declarations	

Declarations

Acknowledgments

The authors thank AC and MW for review and revision and long-term spurs. We also thank AC and MW for their motivation in the experimental process of this paper.

Author contributions

LY and XH conceived, designed and performed most experiments; analysed the data; and drafted the manuscript. AC and MW conceived and supervised the study. RJ,QY, YW, SC, ML, DZ, XO, XW, SM, DS, SZ, XZ, JH, QG, YL, YY, LZ, BT, LP, RU and XC interpreted the data. All authors read and approved the final manuscript for publication.

Funding

This work was supported by the National Key Research and Development Program of China (2017YFD0500800), the China Agricultural Research System (CARS-42-17), the Sichuan Veterinary Medicine and Drug Innovation Group of China Agricultural Research System (CARS-SVDIP) and Integration and Demonstration of Key Technologies for Goose Industrial Chain in Sichuan

Province (2018NZ0005). The funders supervised of the study and did not have any role in the collection, analysis, and interpretation of data or in writing the manuscript.

Availability of data and materials

The datasets used and/or analyzed during the current study are available from the corresponding author on reasonable request.

Ethics approval and consent to participate

The study was approved by the Committee of Experiment Operational Guidelines and Animal Welfare of Sichuan Agricultural University. The experiments were conducted in accordance with approved guidelines.

Consent for publication

Not applicable.

Competing interest

The authors have no competing interests to declare.

References

1. Qi X, Cheng A, Wang M, Zhu D, Jia R. The Pathogenesis of Duck Virus Enteritis in Experimentally Infected Ducks: A Quantitative Time-Course Study Using TaqMan Polymerase Chain Reaction. Avian Pathology. 2008; 37, 307-10.
2. Yuan G, Cheng A, Wang M, Liu F, Han X, Liao Y. et al. Preliminary study on duck enteritis virus-induced lymphocyte apoptosis in vivo. Avian Dis. 2007; 51:546–9.
3. Qi X, Yang X, Cheng A, Wang M, Zhu D, Jia R. et al. Intestinal mucosal immune response against virulent duck enteritis virus infection in ducklings. Res Vet Sci. 2009; 87:218–25.
4. Liu T, Cheng A, Wang M, Jia R, Yang Q, Wu Y. et al. RNA-seq comparative analysis of Peking ducks spleen gene expression 24 h post-infected with duck plague virulent or attenuated virus. Vet Res. 2017; 48:47.
5. King A, Adams M, Lefkowitz EJ. Virus taxonomy: ninth report of the International Committee on Taxonomy of Viruses. Elsevier. 2012.
6. Cheng A. Duck plague. Beijing, China agriculture press. 2015.
7. Wu Y, Cheng A, Wang M, Yang Q, Zhu D, Jia R. et al. Complete Genomic Sequence of Chinese Virulent Duck Enteritis Virus. J Virol. 2012; 86: 5965-5965.
8. Hu X, Wang M, Chen S, Jia R, Zhu D, Liu M. et al. The duck enteritis virus early protein, UL13, found in both nucleus and cytoplasm, influences viral replication in cell culture. Poult Sci. 2017; 96(8):2899-2907.
9. Lee CP, Huang Y, Lin S, Chang Y, Chang Y, Takada, K. et al. Epstein-Barr virus BGLF4 kinase induces disassembly of the nuclear lamina to facilitate virion production. J virol. 2008; 82(23): 11913-11926.
10. Marschall M, Marzi A, aus dem Siepen P, Jochmann R, Kalmer M, Auerochs S. et al. Cellular p32 recruits cytomegalovirus kinase pUL97 to redistribute the nuclear lamina. J Biol Chem. 2005; 280(39): 33357-33367.
11. Krosky P, Baek MC, Coen DM. The human cytomegalovirus UL97 protein kinase, an antiviral drug target, is required at the stage of nuclear egress. J virol. 2003; 77(2): 905-914.
12. Prichard MN, Britt WJ, Daily SL, Hartline CB, Kern ER. Human cytomegalovirus UL97 kinase is required for the normal intranuclear distribution of pp65 and virion morphogenesis. J virol. 2005, 79(24): 15494-15502.
13. Cano-Monreal GL, Wylie KM, Cao F, Tavis JE, Morrison LA. Herpes simplex virus 2 UL13 protein kinas disrupts nuclear lamins. Virology. 2009; 392(1):137-147.
14. Akihisa K, Yamamoto M, Ohno T, Tanaka M, Sata T, Nishiyamaet Y. et al. Herpes simplex virus 1-encoded protein kinase UL13 phosphorylates viral Us3 protein kinase and regulates nuclear localization of viral envelopment factors UL34 and UL31. J Virol. 2006; 80(3): 1476-1486.

15. Marschall M, Freitag M, Suchy P, Romaker D, Kupfer R, Hanke M. et al. The protein kinase pUL97 of human cytomegalovirus interacts with and phosphorylates the DNA polymerase processivity factor pUL44. Virology. 2003; 311(1): 60-71.
16. Yang P, Chang S; Tsai C, Chao Y, Chen M. Effect of phosphorylation on the transactivation activity of Epstein-Barr virus BMRF1, a major target of the viral BGLF4 kinase. J Gen Virol. 2008; 89(4): 884-895.
17. Tarakanova VL, Leung-Pineda V, Hwang S, Yang C, Matatall K, Basson M. et al. γ-herpesvirus kinase actively initiates a DNA damage response by inducing phosphorylation of H2AX to foster viral replication. Cell host microbe. 2007; 1(4): 275-286.
18. Baek MC, Krosky PM, Pearson A, Coen DM. Phosphorylation of the RNA polymerase II carboxyl-terminal domain in human cytomegalovirus-infected cells and in vitro by the viral UL97 protein kinase. Virology. 2004; 324(1):184-193.
19. Tamrakar S, Kapasi AJ, Spector DH. Human cytomegalovirus infection induces specific hyperphosphorylation of the carboxyl-terminal domain of the large subunit of RNA polymerase II that is associated with changes in the abundance, activity, and localization of cdk9 and cdk7. J virol. 2005; 79(24): 15477-15493.
20. Paladino P, Marcon E, Greenblatt J, Frappier L. Identification of herpesvirus proteins that contribute to G1/S arrest. J virol. 2014; 88(8):4480-4492.
21. Chang YH, Lee CP, Su M, Wang J, Chen J, Lin S. et al. Epstein-Barr virus BGLF4 kinase retards cellular S-phase progression and induces chromosomal abnormality. PloS one. 2012; 7(6): e39217.
22. Hwang S, Kim KS, Flano E, Wu T, Tong LM, Park AN. et al. Conserved herpesviral kinase promotes viral persistence by inhibiting the IRF-3-mediated type I interferon response. Cell host microbe. 2009; 5(2):166-178.
23. Wang J, Doong SL, Teng SC, Lee CP, Tsai CH, Chen MR. Epstein-Barr virus BGLF4 kinase suppresses the interferon regulatory factor 3 signaling pathway. J virol. 2009; 83(4): 1856-1869.
24. Yokota S, Yokosawa N, Okabayashi T, Suzutani T, Miura S, Jimbow K. et al. Induction of suppressor of cytokine signaling-3 by herpes simplex virus type 1 contributes to inhibition of the interferon signaling pathway. J virol. 2004; 78(12): 6282-6286.
25. Littler E, Stuart AD, Chee MS. Human cytomegalovirus UL97 open reading frame encodes a protein that phosphorylates the antiviral nucleoside analogue ganciclovir. Nature.1992; 358: 160-162.
26. Michel D, Schaarschmidt P, Wunderlich K, Heuschmid M, Simoncini L, Mühlberger D. et al. Functional regions of the human cytomegalovirus protein pUL97 involved in nuclear localization and phosphorylation of ganciclovir and pUL97 itself. J Gen virol. 1998; 79(9): 2105-2112.
27. Leen D, Bolle DM, Mertens T, Manichanh C, Agut H, Clercq ED. et al. Role of the Human Herpesvirus 6 U69-Encoded Kinase in the Phosphorylation of Ganciclovir. Mol Pharmacol. 2002; 62(3):714-721.
28. Cannon JS, Hamzeh F, Moore S, Nicholas J, Ambinder RF. Human herpesvirus 8-encoded thymidine kinase and phosphotransferase homologues confer sensitivity to ganciclovir. J virol. 1999; 73(6):4786-4793.
29. Meng Q, Hagemeier SR, Fingeroth JD, Gershburg E, Pagano JS, Kenney SC. The Epstein-Barr virus (EBV)-encoded protein kinase, EBV-PK, but not the thymidine kinase (EBV-TK), is required for ganciclovir and acyclovir inhibition of lytic viral production. J virol. 2010; 84(9):4534-4542.
30. Zhou X, Wang M, Cheng A, Yang Q, Wu Y, Jia R. et al. Development a simple and rapid immunochromatographic strip test for detecting antibody of duck plague virus based on gI protein. J Virol Method. 2020; 277: 113803, doi: org/10.1016/j.jviromet.2019.113803.
31. Yang L, Wang M, Zeng C, Shi Y, Cheng A, Liu M. et al. Duck enteritis virus UL21 is a late gene and encodes a protein that interacts with pUL16. BMC Vet Res. 2020;16:8.
32. Zhao C, He T, Xu Y, Wang M, Cheng A, Zhao X. et al. Molecular characterization and antiapoptotic function analysis of the duck plague virus Us5 gene. Sci Rep. 2019; 9:4851.
33. Ma Y, Zeng Q, Wang M, Cheng A, Jia R, Yang Q. et al. US10 Protein Is Crucial but not Indispensable for Duck Enteritis Virus Infection in Vitro. Sci Rep. 2018; 8 (1), 16510.
34. Feng D, Cui M, Jia R, Liu S, Wang M, Yang Q. et al. Co-localization of and Interaction between Duck Enteritis Virus Glycoprotein H and L. BMC Vet Res. 2018; 14 (1), 255.
35. You Y, Liu T, Wang M, Cheng A, Jia R, Yang Q. et al. Duck plague virus Glycoprotein J is functional but slightly impaired in viral replication and cell-to-cell spread. Sci Rep. 2018; 8(1):4069.

36. Yang L, Wang M, Cheng A, Yang Q, Wu Y, Jia R. et al. Innate immune evasion of alphaherpersvirus tegument proteins. Front immunol. 2019; 10:2196.
37. Jing Y, Wu Y, Sun K, Wang M, Cheng A, Chen S. et al. Role of duck plague virus glycoprotein C in viral adsorption: Absence of specific interactions with cell surface heparan sulfate. Journal of Integrative Agriculture. 2017; 16(5): 1145-1152.
38. Liu C, Cheng A, Wang M, Chen S, Jia R, Zhu D. et al. Regulation of viral gene expression by duck enteritis virus UL54. Sci Rep. 2017; 7(1): 1076.
39. Wu Y, Li Y, Wang M, Sun K, Jia R, Chen S. et al. Preliminary study of the UL55 gene based on infectious Chinese virulent duck enteritis virus bacterial artificial chromosome clone. Virol J. 2017; 14(1): 78.
40. Gao J, Cheng A, Wang M, Jia R, Zhu D, Chen S. et al. Identification and characterization of the duck enteritis virus (DEV) US2 gene. Genets Mol Res. 2015; 29; 14 (4): 13779-13790.
41. He T, Wang M, Cao X, Cheng A, Wu Y, Yang Q. et al. Molecular characterization of duck enteritis virus UL41 protein. Virol J. 2018; 15:12.
42. Zhang D, Lai M, Wu Y, Yang Q, Liu M, Zhu D. et al. Molecular characterization of the duck enteritis virus US10 protein. Virol J. 2017; 14:183.
43. Liu C, Cheng A, Wang M, Chen S, Jia R, Zhu D. et al. Duck enteritis virus UL54 is an IE protein primarily located in the nucleus. Virol J. 2015;12: 198.
44. Lin M, Jia R, Wang M, Gao X, Zhu D, Chen S. et al. Molecular Characterization of Duck Enteritis Virus CHv Strain UL49.5 protein and its Colocalization with Glycoprotein M. J Vet Sci. 2014; 15(3): 389-39.
45. Sun K, Cheng A, Wang M. Bioinformatic analysis and characteristics of glycoprotein C encoded by the newly identified UL44 gene of duck plague virus. Genet Mol Res. 2014; 13(2): 4505 – 4515.
46. Wang M, Lin D, Zhang S, Zhu D, Jia R, Chen X. et al. Prokaryotic expression of the truncated duck enteritis virus UL27 gene and characteristics of UL27 gene and its truncated product. Acta virol. 2012; 56: 323-28.
47. He Q, Cheng A, Wang M, Xiang J, Zhu D, Zhou Y. et al. Replication kinetics of duck enteritis virus UL16 gene in vitro. Virol J. 2012; 9:281.
48. Xiang J, Zhang S, Cheng A, Wang M, Chang H, Shen C. et al. Expression and characterization of recombinant VP19c protein and N-terminal from Duck Enteritis Virus. Virol J. 2011; 8: 82.
49. Zhang S, Xiang J, Cheng A, Wang M, Wu Y, Yang X. et al. Characterization of duck enteritis virus UL53 gene and glycoprotein K. Virol J. 2011; 8:235
50. Li L, Cheng A, Wang M, Zhang S, Xiang J, Yang X. et al. Expression and Characterization of Duck Enteritis Virus gI Gene. Virol J. 2011; 8:241.
51. He Q, Yang Q, Cheng A, Wang M, Xiang J, Zhu D. et al. Expression and characterization of UL16 gene from duck enteritis virus. Virol J. 2011; 8:413.
52. Xie W, Cheng A, Wang M, Chang H, Zhu D, Luo Q. Molecular cloning and characterization of the UL31 gene from Duck enteritis virus. Mol Bio Rep. 2010;37 (3):1495-1503.
53. Cai M, Cheng A, Wang M, Chen W, Zhang X, Zheng S. et al. Characterization of the duck plague virus UL35 gene. Intervirology. 2010; 53:408-416
54. Lian B, Chao X, Cheng A, Wang M, Zhu D, Luo Q. et al. Identification and characterization of duck plague virus glycoprotein C gene and gene products. Virol J. 2010; 7:349
55. Gao X, Jia R, Wang M, Yang Q, Chen S, Liu M. et al. Duck enteritis virus (DEV) UL54 protein, a novel partner, interacts with DEV UL24 protein. Virol J. 2017;14(1): 166.
56. Li Y, Wu Y, Wang M, Ma Y, Jia R, Chen S. et al. Duplicate US1 genes of duck enteritis virus encode a non-essential immediate early protein localized to the nucleus. Front Cell Infect Microbiol. 2020; 9, 463.
57. Thary J, Céline Van den B, Herman WF. Viral serine/threonine protein kinases. J virol. 2011; 85(3): 1158-1173.
58. Schumacher D, Tischer BK, Trapp S, Osterrieder N. The protein encoded by the US3 orthologue of Marek's disease virus is required for efficient de-envelopment of perinuclear virions and involved in actin stress fiber breakdown. J Virol. 2005; 79(7):3987.

59. Anne S, Fortin JF, Sommer M, Zerboni L, Stamatis S, Ku C. et al. T-cell tropism and the role of ORF66 protein in pathogenesis of varicella-zoster virus infection. J Virol. 2005; 79(20):12921.
60. Eisfeld AJ, Turse SE, Jackson SA, Lerner EC, Kinchington PR. Phosphorylation of the varicella-zoster virus (VZV) major transcriptional regulatory protein IE62 by the VZV open reading frame 66 protein kinase. J Virol. 2006; 80(4):1710.
61. Erazo A, Kinchington PR. Varicella-Zoster Virus Open Reading Frame 66 Protein Kinase and Its Relationship to Alphaherpesvirus US3 Kinases. Curr Top Microbiol Immunol. 2010; 342:79-98.
62. Ng TI, Keenan L, Kinchington PR, Grose C. Phosphorylation of varicella-zoster virus open reading frame (ORF) 62 regulatory product by viral ORF 47-associated protein kinase. J Virol. 1994; 68(3):1350.
63. Krosky PM, Moon-Chang B, Coen DM. The Human Cytomegalovirus UL97 Protein Kinase, an Antiviral Drug Target, Is Required at the Stage of Nuclear Egress. J Virol. 2003; 77(2): 905-914.
64. Chen M, Chang S, Huang H, Chen J. A protein kinase activity associated with Epstein-Barr virus BGLF4 phosphorylates the viral early antigen EA-D in vitro. J Virol. 2000; 74(7):3093-3104.
65. Purves F, Ogle W, Roizman B. Processing of the herpes simplex virus regulatory protein α22 mediated by the UL13 protein kinase determines the accumulation of a subset of α and γ mRNAs and proteins in infected cells. Proc Natl Acad Sci U S A. 1993; 90(14): 6701-6705.
66. Reynolds AE, Wills EG, Roller RJ, Ryckman BJ, Baines JD. Ultrastructural localization of the herpes simplex virus type 1 UL31, UL34, and US3 proteins suggests specific roles in primary envelopment and egress of nucleocapsids. J Virol. 2002; 76(17):8939-8952.
67. Zhao L, Cheng A, Wang M, Yuan G, Cai M. Characterization of codon usage bias in the dUTPase gene of duck enteritis virus. Progress in Natural Science. 2008; 18(8):1069-1076.
68. Chang H, Cheng A, Wang M, Guo Y, Xie W, Luo Q. Complete nucleotide sequence of the Duck plague virus gE gene. Arc Virol. 2009; 154(1): 163-165.
69. Nakai, K.; Horton, P. PSORT: a program for detecting sorting signals in proteins and predicting their subcellular localization. Trends in Biochemical Sciences. 1999, 24(1):34-36.
70. Jia R, Cheng A, Wang M, Qi X, Zhu D, Ge H. et al. Development and evaluation of an antigen-capture ELISA for detection of the UL24 antigen of the duck enteritis virus, based on a polyclonal antibody against the UL24 expression protein. J Virol Methods. 2009; 161: 38–43.
71. Xie W, Cheng A, Wang M, Chang H, Zhu D, Luo Q. et al. Expression and characterization of the UL31 protein from duck enteritis virus. Virol J. 2009; 6:19.
72. Shen C, Guo Y, Cheng A, Wang M, Zhou Y, Lin D. et al. Characterization of subcellular localization of duck enteritis virus UL51 protein. Virol J. 2009; 6:92.
73. Jia R, Wang M, Cheng A, Zhu D, Ge H, Xin H. et al. Cloning, expression, purification and characterization of UL24 protein of Partial duck enteritis virus. Intervirology. 2009; 52:326-334.
74. Xin H, Cheng A, Wang M, Jia R, Shen C, Chang H. Identification and characterization of a duck enteritis virus US3-like gene. Avian Dis. 2009; 53(3): 363-370.
75. Zhang S, Xiang J, Cheng A, Wang M, Li X, Li L. et al. Production, purification and characterization of polyclonal antibody against the truncated gK of the duck enteritis virus Virol J. 2010; 7:241.
76. Chang, H.; Cheng, A.C.; Wang, M.S.; Jia, R.Y.; Zhu, D.K.; Luo, Q.H.; Chen, Z.L.; Zhou, Y.; Liu, F.; Chen, X.Y. Immunofluorescence Analysis of Duck plague virus gE protein on DPV-infected ducks. Virol J. 2011, 8:19.
77. Zhang S, Cheng A, Wang M. Characteristics and functional roles of glycoprotein K of herpesviruses. Reviews in Medical Microbiology. 2011; 22(4):90–95.
78. Guo Y, Cheng A, Wang M, Zhou Y. Purification of anatid herpesvirus 1 particles by tangential-flow ultrafiltration and sucrose gradient ultracentrifugation. J Virol Methods. 2009; 161(1):1-6.
79. Chang H, Cheng A, Wang M, Zhu D, Jia R, Liu F. et al. Cloning, Expression and Characterization of gE protein of Duck plague virus. Virol J. 2010; 7:120.

80. Shen A, Ma G, Cheng A, Wang M, Luo D, Lu L. et al. Transcription phase,protein characteristics of DEV UL45 and prokaryotic expression, antibody preparation of the UL45 des-transmembrane domain. Virol J. 2010; 7:232
81. Wagstaff KM, Sivakumaran H, Heaton SM, Harrich D, Jans DA. Ivermectin is a specific inhibitor of importin alpha/beta-mediated nuclear import able to inhibit replication of HIV-1 and dengue virus. Biochem J. 2012; 443(3):851-856.
82. Nishi K, Yoshida M, Fujiwara D, Nishikawa M, Horinouchi S, Beppu T. Leptomycin B targets a regulatory cascade of crm1, a fission yeast nuclear protein, involved in control of higher order chromosome structure and gene expression. J Bio Chem. 1994; 269(9):6320-6324.
83. Kudo N, Wolff B, Sekimoto T, Schreiner EP, Yoneda Y, Yanagida M. et al. Leptomycin B inhibition of signal-mediated nuclear export by direct binding to CRM1. Exp Cell Res. 1998; 242(2):540-547.
84. Guo Y, Shen C, Cheng A, Wang M, Chen S, Zhang N. et al. Anatid herpesvirus 1 virulent strain induces syncytium and apoptosis in duck embryo fibroblast cultures. Vet Microbiol. 2009;138:258-265.
85. Yuan G, Cheng A, Wang M, Han X, Zhou Y, Liu F. Preliminary Study on Duck Enteritis Virus-Induced Lymphocyte Apoptosis In Vivo. Avian dis. 2007; 51(2):546–549.
86. Liu C, Cheng A, Wang M, Chen S, Jia R, Zhu D. et al. Characterization of nucleocytoplasmic shuttling and intracellular localization signals in Duck Enteritis Virus UL54. Biochimie. 2016;127: 86–94.

Additional Files

Additional file 1. Figure S1. Online prediction of UL13 nuclear positioning signal through PSORT II. UL13 has two nuclear positioning signals.

Figures

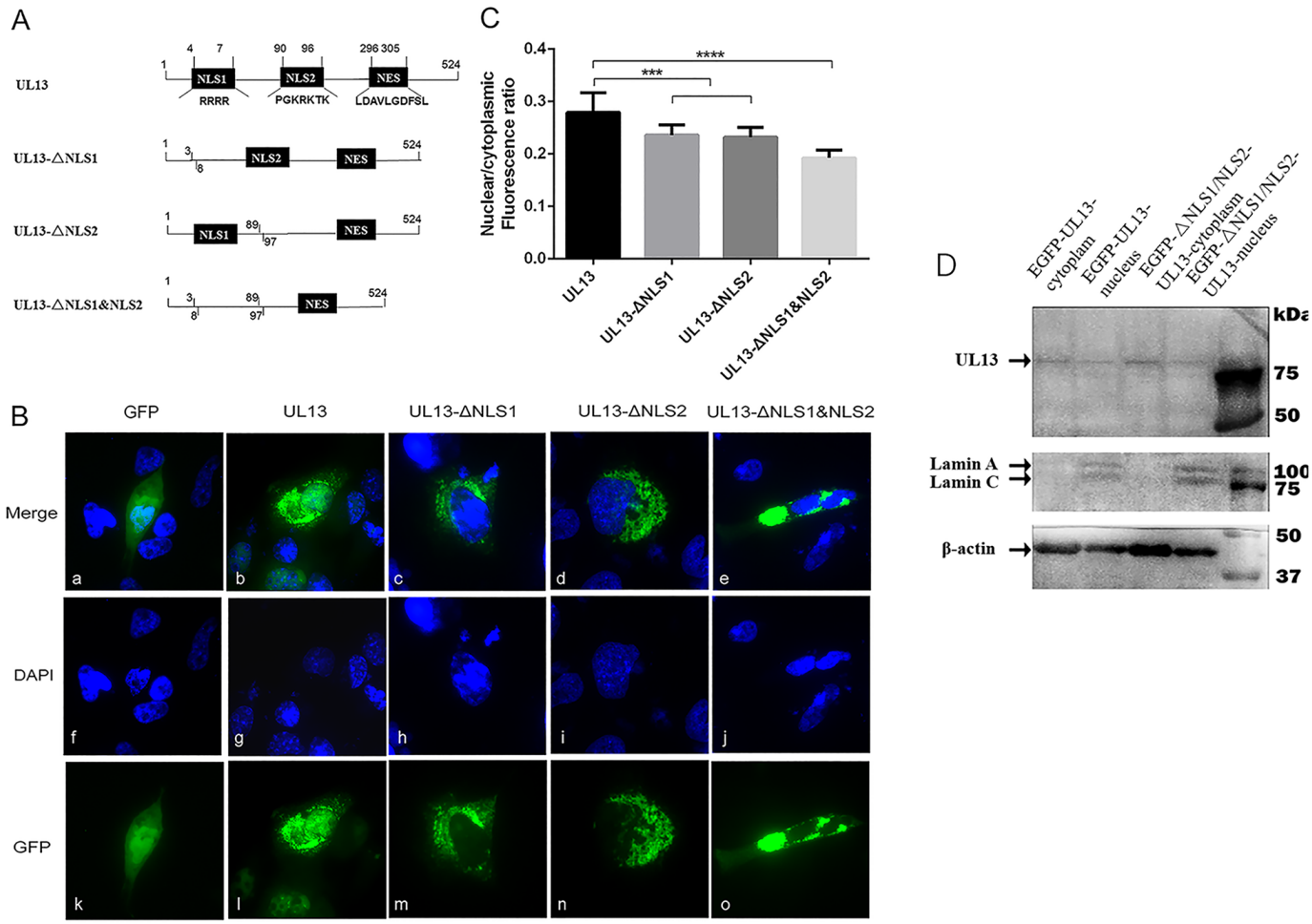

Figure 1

Localization of the UL13 and UL13-△NLS proteins in transfected DEFs. (A) Sketch map of the construction of UL13 with NLS deletion related recombinant plasmids. (B) Verification of UL13/UL13-△NLS fusion protein localization via IFA. Plasmids of pEGFP-N1- UL13/UL13-△NLS were transfected into DEF cells. At 16h post-transfection, the cells were fixed, permeabilized and incubated with rabbit anti-UL13 antiserum. Nuclei were stained with DAPI (blue). The expression and distribution of GFP protein (green) was monitored by fluorescence microscopy. Images were recorded in separate channels using a ×40 objective and merged in SPOT software. (C) The nuclear/cytoplasmic fluorescence ratio analysis. The ratio of nuclear and cytoplasmic distribution of fluorescence in the recombinant plasmid transfection group was calculated by Image Pro Plus. The number of cells was 50 in each group. The difference of the ratio of nuclear and cytoplasmic fluorescence in the pEGFP-UL13-ΔNLS1, pGFP-UL13-ΔNLS2 and pGFP-UL13-ΔNLS1 & ΔNLS2 recombinant plasmid transfection group was analyzed by graphpad prism 6.0 software. *P < 0.05 **P < 0.01.(D) The nuclear/cytoplasmic distribution of UL13 protein after the deletion of NLS1 and NLS2 through western blot.

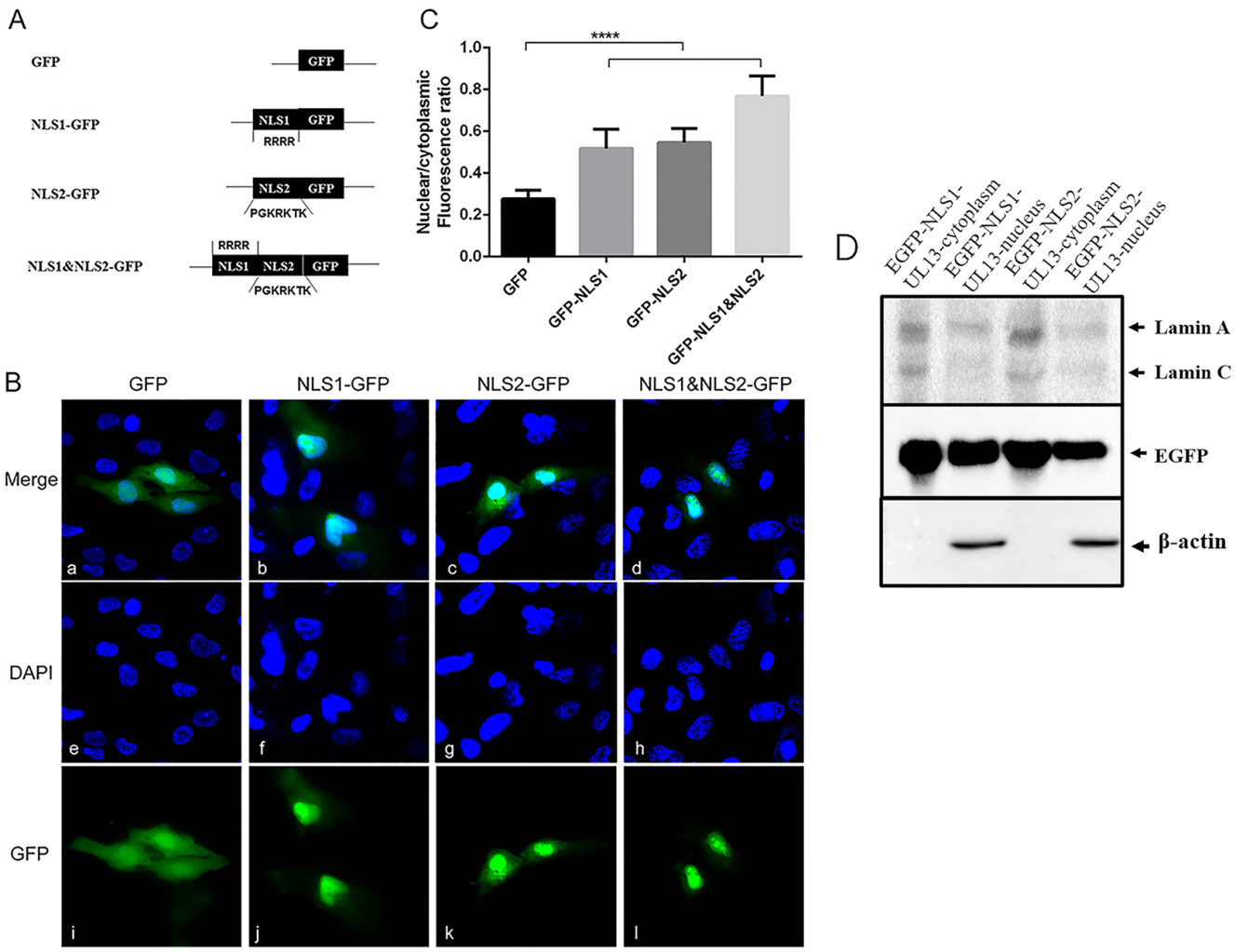

Figure 2

Construction of NLSs-GFP recombinant plasmids and localization analysis of the fusion proteins. (A) Sketch map of the construction of UL13 with NLS fusion protein recombinant plasmids. (B) Localization of the NLS-GFP fusion proteins in transfected DEFs. NLS-GFP recombinants were transfected into DEF cells, which were then fixed at 16h post-transfection. Images of the GFP reporter (green) and nuclei stained with DAPI (blue) were recorded in separate channels using a ×40 objective and merged in SPOT software. (C) Comparison of the nuclear and cytoplasmic fluorescence ratios between GFP and NLS-GFP fusion proteins. Mean nuclear and cytoplasmic fluorescence ratios were quantified using Image-Pro Plus software; analysis of the differences in the nuclear and cytoplasmic fluorescence ratios between GFP and the NLS1-GFP/NLS2-GFP/ NLS1&NLS2-GFP proteins was performed using ANOVA with GraphPad Prism 6.0 software. N=50 for each group. (D) The nuclear/cytoplasmic distribution of UL13 NLS1 and NLS2 through western blot.

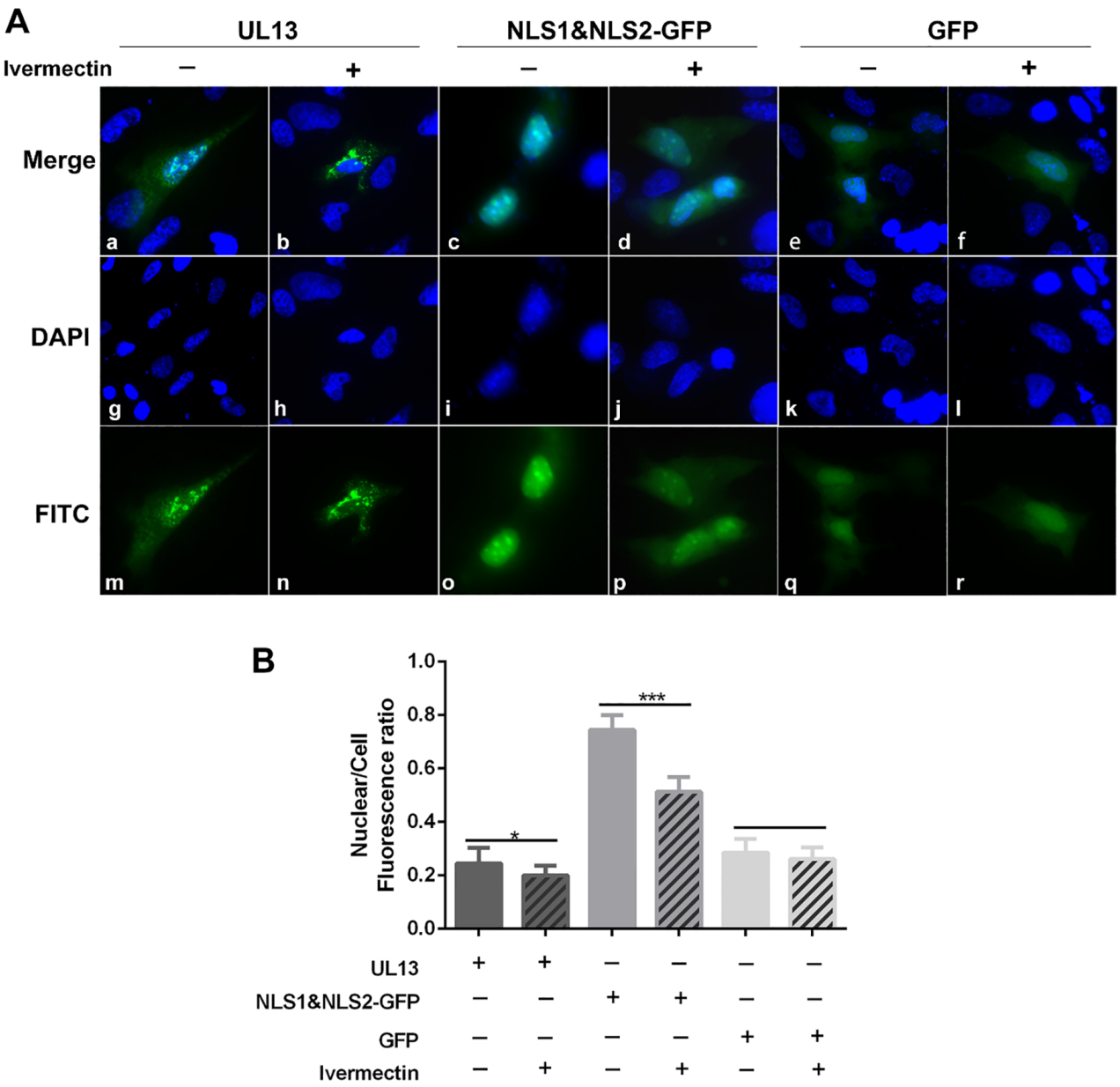

Figure 3

The effects of nuclear import inhibitors on the location of DEV UL13 protein assay. (A) Location of UL13-GFP/ NLS1&NLS2-GFP protein with or without ivermectin treatment. At 16h post-transfection, 25 μM ivermectin was added 1 h before fixation. Images of the GFP reporter (green) and nuclei stained with DAPI (blue) were recorded in separate channels using a ×40 objective and merged in SPOT software. (B) Comparison of the nuclear and cytoplasmic fluorescence ratios between proteins with or without ivermectin treatment. Mean nuclear and cytoplasmic fluorescence ratios were quantified using Image-Pro Plus software; analysis of the differences in the nuclear and cytoplasmic fluorescence ratios of UL13-GFP/ NLS1&NLS2-GFP protein with or without ivermectin treatment was performed using ANOVA with GraphPad Prism 6.0 software. N=50 for each group.

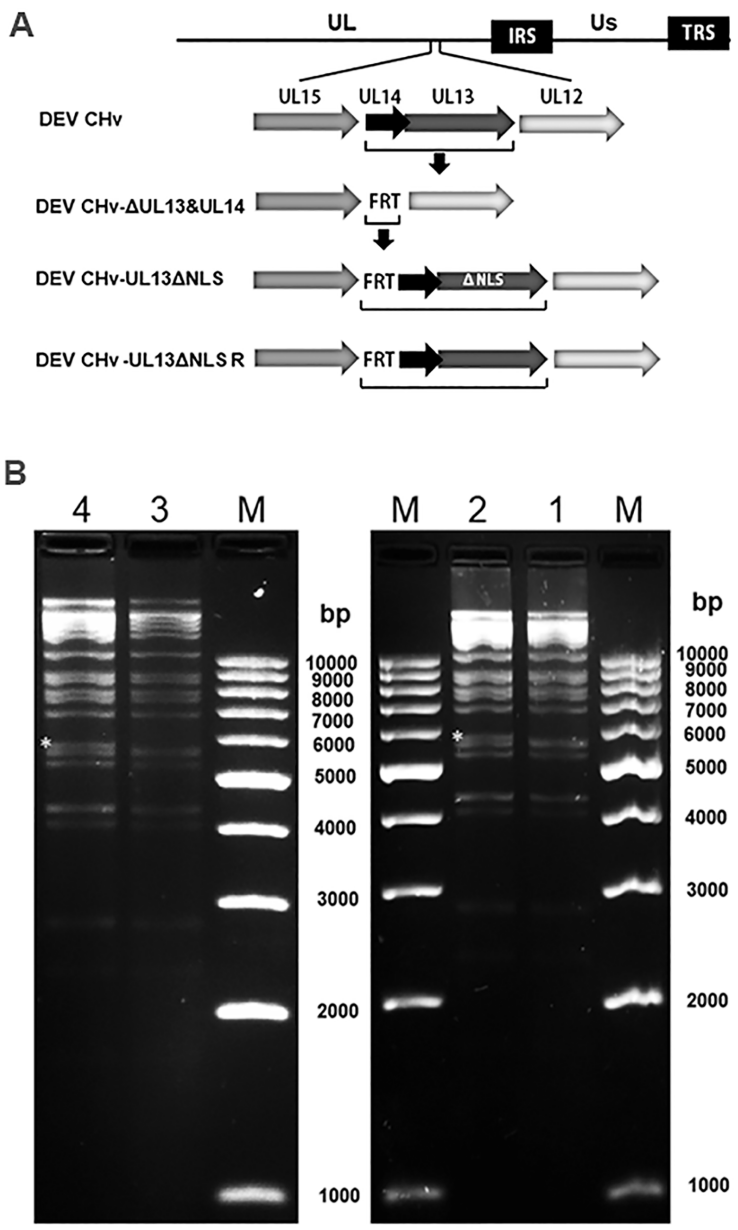

Figure 4

Construction and identification of DEV CHv-ΔUL13 and DEV CHv-ΔUL13R recombinant viruses. (A) Schematic representation of the DEV genome in the UL13 region and part of the sequence for DEV CHv-UL13ΔNLS and the repaired DEV CHv-UL13ΔNLS R. (B) RFLP analysis. Lane 1 and lane 3, DEV CHv -G plasmids were digested with SalI restriction endonuclease; Lane 2, DEV CHv-UL13ΔNLS-G plasmids were digested with SalI restriction endonuclease; Lane 4, DEV CHv-UL13ΔNLS R-G plasmids were digested with SalI restriction endonuclease. Digestion of the deletion and revertant products caused the size of the 5,714 bp fragment of the parental virus (Lane 1 and lane 3) to change to 5,765 bp and 5,798 bp (Lane 2 and Lane 4), respectively. No extraneous alterations were evident in either clone. M, 1 kb plus DNA ladder. ∗: Different band.

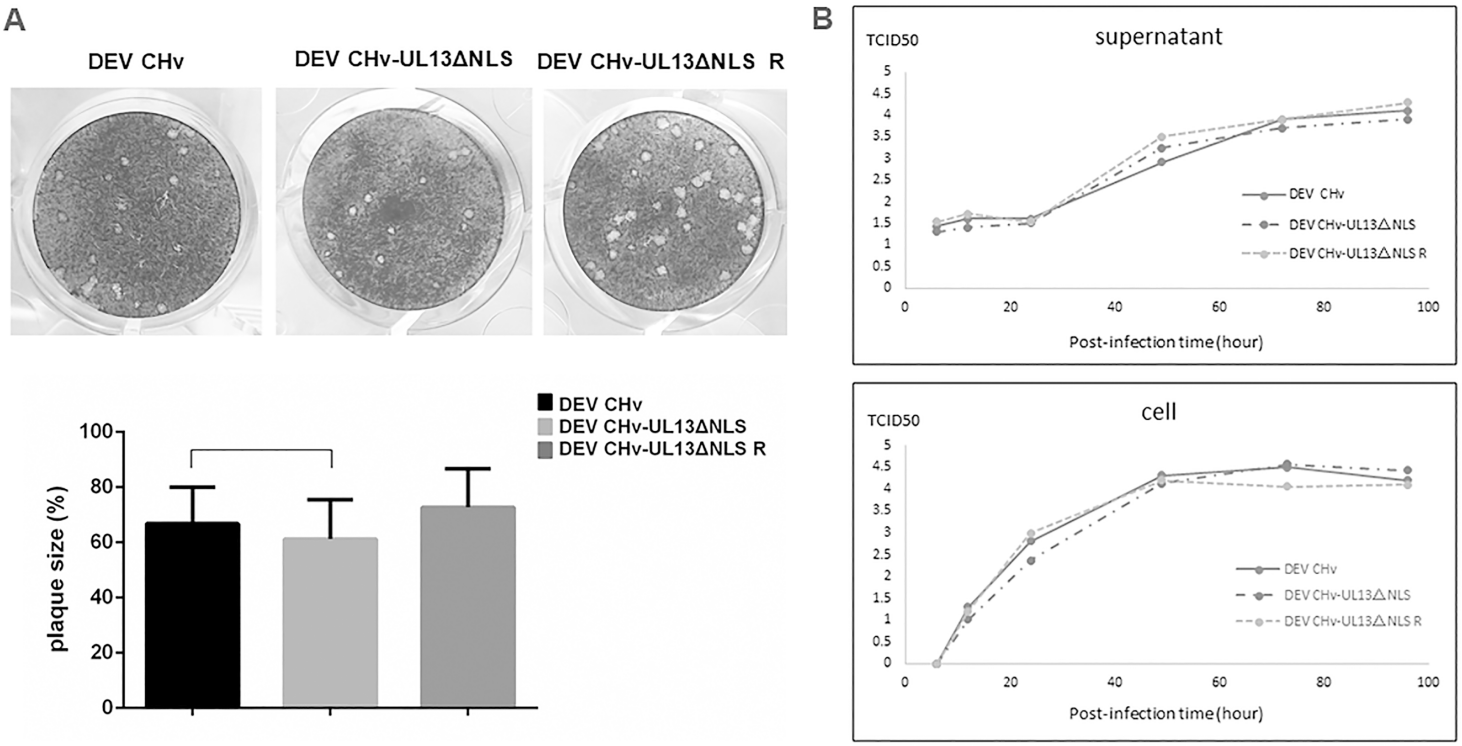

Figure 5

Analysis of the characteristics of the UL13-deletion mutant virus in cell culture. (A) Plaque assay. The upper figures represent the phenotypes of the plaques formed by DEV CHv, DEV CHv-UL13ΔNLS, and DEV CHv-UL13ΔNLS R virus infection; the lower figure shows the analysis of the mean areas of the viral plaques formed by the various viruses during infection. The digital images were analyzed using Image-Pro Plus software and the statistical analyses were performed using GraphPad Prism 6.0 software. (B) Growth curve. DEF were infected with DEV CHv, DEV CHv-UL13ΔNLS, and DEV CHv-UL13ΔNLS R at a titer of 200 TCID50 and harvested at 6, 12, 24, 48, 72, and 96h post infection. The curves were generated based on the titers of the different harvests, by testing for the TCID50 using Excel. And the significant difference analyses between DEV CHv and DEV CHv -ΔUL13 were performed using GraphPad Prism 6.0 software.

Supplementary Files

This is a list of supplementary files associated with this preprint. Click to download.

- Supplementarydatas.docx